

Technical Notes

TECHNICAL NOTES are short manuscripts describing new developments or important results of a preliminary nature. These Notes cannot exceed 6 manuscript pages and 3 figures; a page of text may be substituted for a figure and vice versa. After informal review by the editors, they may be published within a few months of the date of receipt. Style requirements are the same as for regular contributions (see inside back cover).

Electromagnetic Attenuation in Plasmas Generated by Atmospheric Flight

Michael J. Nusca*

U.S. Army Research Laboratory,
Aberdeen Proving Ground, Maryland 21005

Nomenclature

| | |
|------------|-------------------------------------|
| B | = magnetic field strength |
| E | = electric field strength |
| e | = electron charge |
| j | = current density |
| k | = Boltzmann constant |
| M | = molecular weight |
| m | = mass |
| n | = number density |
| Q | = excess charge density |
| T | = gas temperature |
| W | = signal power or wave amplitude |
| y | = surface-normal coordinate |
| γ | = ratio of specific heats |
| δ | = plasma-layer thickness |
| ϵ | = permittivity constant |
| λ | = signal wavelength |
| μ | = plasma permeability |
| ϕ | = collision frequency in the plasma |
| ω | = signal frequency |

Subscripts

| | |
|-------|--------------------------|
| e_l | = electron property |
| in | = incident wave property |
| p | = plasma property |

Introduction

HYPERVELOCITY flight in the atmosphere can cause chemical dissociation in the vehicle shock layer, generating ions and electrons that can shroud the vehicle in a thin, highly stratified layer of plasma. Electromagnetic (EM) signals, transmitted to and from the vehicle, must propagate through the plasma layer and are attenuated. There are several important physical phenomena associated with high-speed atmospheric flight that affect the flowfield properties in the vicinity of the vehicle and have an ultimate effect on EM wave propagation. Among these are shock and stagnation heating that excites vibrational energy modes and causes chemical reaction, strong species diffusion in the viscous layer resulting from concentration and thermal gradients, freezing of non-

equilibrium electron concentration caused by rapid flow expansion around the vehicle, and catalytic wall effects. Plasma layers generated aerodynamically are generally thin (relative to λ) and are weakly ionized. Since the plasma layer is thin, the time interval of interaction between the EM wave and the electrons is very small. Electrons are given an oscillatory motion by this interaction, but this motion is about unaltered electron trajectories; the EM wave and the free electrons exchange of energy and W is reduced, i.e., the signal is attenuated (see Ref. 1 for a discussion of attenuation). Theoretical studies of EM wave attenuation generally treat a plasma layer as a dielectric material with a variable μ distribution.^{2,3} In the present study computational fluid dynamics (CFD), based on the Navier–Stokes equations, is used to determine the properties of the chemically reacting flowfield including layers of free electrons (plasmas), whereas computational EMs, based on Maxwell's equations, is used to compute signal attenuation.

Gasdynamic Analysis

A hypervelocity flowfield can be numerically simulated using CFD based on the Navier–Stokes equations for chemical/thermal nonequilibrium. The ARL–NSRG2 CFD code includes species diffusion, thermal conduction, viscosity, and nonequilibrium chemical kinetics. An explicit Runge–Kutta algorithm is utilized for time integration. The convective and transport terms are resolved using centered differencing. For steady flows, convergence acceleration is used to reduce the numerical stiffness of the discretized equations; for a mesh-constant Courant number the time step is based on the local conditions for each mesh cell. A detailed description of the ARL–NSRG2 code is given by Nusca⁴ for a problem in methane combustion. For air dissociation, considered in the present study, the code includes seven species (O_2 , N_2 , O , N , NO , NO^+ , and e^-), with chemical reaction rates defined by Arrhenius relations and rate data taken from Dunn and Kang.⁵ Species diffusion resulting from thermal and concentration gradients is included. The thermal diffusion factor is given by Chapman and Cowling,⁶ as is the binary diffusion coefficient in terms of the collision cross section and the characteristic Lennard–Jones energy, quantities that are zero for the electron. In a partially ionized gas with no induced electric current (i.e., no charge separation), the electron diffusion velocity is equal to that of ions; the electron diffusion coefficient is determined using the ion coefficient.

Chadwick et al.⁷ measured n_{el} profiles along a blunt metallic cone of 7.8-deg, half-angle, 0.043-m nose radius, and about 1 m in length, mounted in a hypersonic shock tunnel. Flow conditions upstream of the cone corresponded to an altitude of about 43 km and the freestream velocity was 4229 m/s (Mach number of 9.3) with a unit Reynolds number of 0.14×10^6 . The mass fractions of O_2 and N_2 in the freestream were approximately 0.233 and 0.767, respectively ($M = 28.7$, $\gamma = 1.39$). For the numerical simulation the computational domain extends 0.061 m ahead of the nosetip, 0.914 m along the cone, and 0.325 m above the cone centerline with a grid consisting of 199 axial and 220 radial cells clustered near the cone surface (first grid node at $y = 8 \times 10^{-4}$ m). The cone wall is assumed isothermal ($T = 295$ K) and fully catalytic, and the flow is assumed laminar (Lewis number 1.4). Figure 1 shows $n_{el}(y)$ profiles at 20 cm (ES-1) and 47 cm (ES-2) from the

Received Aug. 27, 1996; revision received Oct. 7, 1996; accepted for publication Oct. 7, 1996. This paper is declared a work of the U.S. Government and is not subject to copyright protection in the United States.

*Aerospace Engineer, Weapons and Materials Research Directorate, AMSRL-WM-PA. Associate Fellow AIAA.

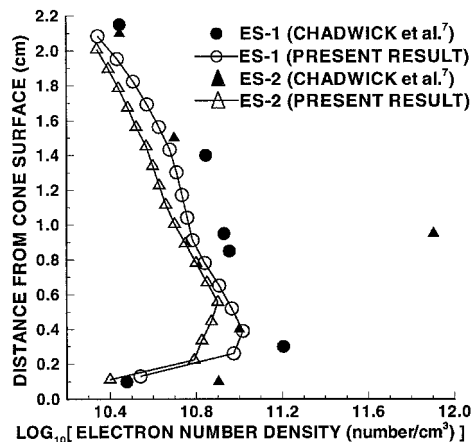


Fig. 1 Electron number density profiles for nonequilibrium cone flow at 20 cm (ES-1) and 47 cm (ES-2) from the nosetip.

nosetip. The maximum discrepancy of 30% between measured and computed values, for the ES-1 position, occurs at the peak number density ($y = 0.2$ cm). The computed profile for the ES-2 position is similar to that for ES-1 with the location of peak density occurring at $y = 0.5$ cm.

EM Analysis

EM wave attenuation in an ionized flow is treated using the theory of wave propagation through a continuous plasma medium with properties $n_{el}(y)$, $\phi(y)$, and $T_{el}(y)$ determined from gasdynamics analysis. The ionized flowfield is treated as a plasma consisting of an equal number of electrons and ions mixed with neutral particles. An estimate of the minimum distance over which a gas mixture is considered a plasma is $L = [9\epsilon kT/(e^2 n_{el})]^{1/2}$ (Ref. 8). Except for a numerical factor (i.e., $\sqrt{9}$), L is the Debye length. For high Mach number flows, L (typically ≤ 0.01 mm) is much smaller than relevant flow dimensions of the ionized gas; e.g., the shock-layer thickness. Shen and Qu⁹ showed that the nonequilibrium air shock layer about a hypervelocity vehicle is grossly electric neutral since a slight separation of charges induces a strong electric field that prevents further separation. The energy in an EM wave propagating through the plasma layer is partially absorbed by electrons and partially reflected by the plasma boundary. Effectively, complete wave transmission (i.e., no attenuation) occurs only at wave frequencies ω much greater than ω_p , the plasma frequency.¹ For $\omega < \omega_p$, the attenuation depends on ω , λ , and on n_{el} , δ , and ϕ for the plasma. The larger ω_p/ω and/or δ/λ , the higher the attenuation.

The equations of Maxwell describe the space-time variation of an EM field and a magnetic field. Marion and Heald¹⁰ show that in a conducting medium, each field satisfies identical wave equations. Since the plasma layer is thin and weakly ionized⁸ (i.e., $n_{el}/(n - n_{el}) < 10^{-4}$), the induced B , because of the movement of electrons in the plasma, is negligible. Therefore, without an applied magnetic field, $B = 0$. Since the plasma is electrically neutral, $Q = 0$. It is assumed that the plasma layer is confined to the shock layer, δ is constant where the EM wave transverses the plasma, plasma properties vary only in the y direction, and the EM wave is a plane wave incident normal to the plasma layer. Thus, the wave equation for E becomes

$$\frac{\partial^2 E}{\partial y^2} = 4\pi\mu \frac{\partial j}{\partial t} + \epsilon\mu \frac{\partial^2 E}{\partial t^2} \quad (1)$$

where, $E = W \exp(-i\omega t)$ and μ is a function of n_{el} , ω , and ϕ (ϕ is related to T_{el}). For thermal equilibrium, $T_{el} = T$.

Epstein¹¹ developed a solution for Eq. (1) using an infinite series, and approximated this series using the first two terms, appropriate for a thin layer (i.e., small δ/λ). Transmission and

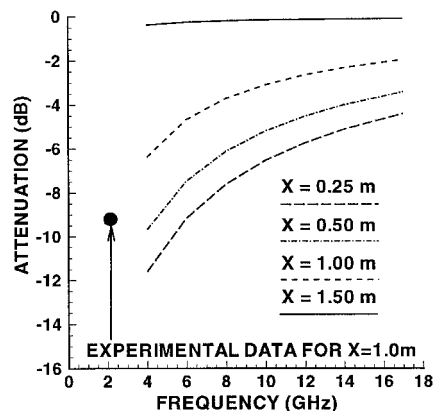


Fig. 2 Variation of attenuation with signal frequency and location from the source (X) using the present method, compared to experimental data at 1.575 GHz.

reflection coefficients are computed from the properties of the plasma layer using algebraic expressions (see Ref. 11). The signal emerging from the plasma layer has power W_{out} , and W_{out}/W_{in} is the transmission coefficient; for decibels of attenuation $\text{dB} = -10 \log_{10}(W_{out}/W_{in}) = 10 \log_{10}(W_{in}/W_{out})$.

Ohler et al.¹² measured signal attenuation for $1.5 \leq \omega \leq 17$ GHz resulting from passage through the plume of a stationary plasma thruster (SPT). The present EM analysis is used for a static SPT plasma layer with measured n_{el} profiles¹² to compute the variation of signal attenuation with distance from the SPT. The computations shown in Fig. 2 demonstrate a trend of decreased attenuation (i.e., $\text{dB} \rightarrow 0$) with increasing distance from the SPT, caused by a decrease in n_{el} , and increasing signal attenuation (i.e., $\text{dB} < 0$) as ω is reduced, caused by the critical electron number density $n_{el,crit} = \omega^2 \epsilon m_{el} / e^2$, decreasing to a value well below the peak density in the plasma plume. For example, $n_{el,crit} = 9 \times 10^{16} \text{ m}^{-3}$ for $\omega = 17$ GHz and $n_{el,crit} = 3 \times 10^{15} \text{ m}^{-3}$ for $\omega = 3$ GHz, while $n_{el,pk} = 6 \times 10^{16} \text{ m}^{-3}$ (for 0.25 m). Heald and Wharton¹ show that this situation results in the greatest attenuation. Comparing present results with a ray-tracing model,¹² the greatest difference occurs at higher ω , whereas close agreement results for smaller ω . Both methods show trends toward the measured value and similar overall trends. The present method is therefore considered accurate for $n_{el,pk} > n_{el,crit}$ (i.e., $\omega \leq 8$ GHz, Fig. 2).

Results

Boyer et al.¹³ conducted experimental studies, using a hypersonic shock tunnel, of EM transmission through an air plasma generated by a blunt 20-deg half-angle wedge about 48 cm in length. The tunnel operated with reservoir conditions of 5800 K and 657 atm, and had a nozzle exit to throat diameter ratio of about 54. Species mass fractions near the nozzle exit were reported to be close to those for undissociated air. Flow conditions upstream of the wedge were 4267.2 m/s with an equivalent density altitude of 47.2 km. The EM transmission, $\omega = 1.7$ GHz, originated from an open-ended rectangular waveguide on the wedge surface. Signal attenuation of 9–25 dB was measured using receiving antennas outside the tunnel walls that were made of low-reflectance material.

For the present numerical simulation, the computational grid extends 1.75 cm upstream of the leading edge and 28 cm above the centerplane of the wedge (wake region ignored). The grid consists of 328 axial and 119 vertical cells clustered near the wedge surface (first grid node at $y = 1 \times 10^{-4}$ m). Figure 3 shows $n_{el}(y)$ through the shock layer at the antenna location. These density levels are expectedly higher than those displayed in Fig. 1 for the 7.8-deg cone. The bow shock at this location is at $y = 2.2$ cm. Computations for viscous flow (Lewis number of unity) show a bow shock displaced further from the wedge surface; the shock is smeared over additional grid cells and